Catena 127 (2015) 80–91

Contents lists available at ScienceDirect

Catena

journal homepage: www.elsevier.com/locate/catena

Effects of rainfall intensity on groundwater recharge based on simulated rainfall experiments and a groundwater flow model

Hong Wang [a,e], Jian En Gao [a,b,c,d,*], Meng-jie Zhang [c], Xing-hua Li [d], Shao-long Zhang [d], Li-zhi Jia [a,e]

[a] Institute of Soil and Water Conservation, Chinese Academy of Sciences and Ministry of Water Resources, Yangling, Shaanxi Province, China
[b] Institute of Soil and Water Conservation, Northwest A&F University, Yangling, Shaanxi Province, China
[c] College of Natural Resources and Environment, Northwest A&F University, Yangling, Shaanxi Province, China
[d] College of Water Resources and Architectural Engineering, Northwest A&F University, Yangling, Shaanxi Province, China
[e] University of Chinese Academy of Sciences, Beijing, China

ARTICLE INFO

Article history:
Received 29 July 2014
Received in revised form 4 December 2014
Accepted 7 December 2014
Available online 29 December 2014

Keywords:
MODFLOW
Rainfall intensity
Recharge coefficient
Rainfall experiments

ABSTRACT

It is important that groundwater discharges sustain baseflow to rivers for the ecological basic flow protection. The objective of this study was to assess the impact of rainfall intensity on groundwater regime under the bare slope condition. A three-dimensional finite-difference groundwater flow model (MODFLOW) was constructed and calibrated and combined with simulated rainfall experiments to study this impact. Groundwater recharge coefficients for different rainfall intensities with a constant amount of rainfall (120 mm) were calculated by using PEST-ASP program of MODFLOW. The values decreased from 0.439 to 0.345, 0.327, 0.167, 0.138, 0.076 with rainfall intensities increasing from 45 mm/h to 60/75/90/105/120 mm/h respectively; recharge coefficients were described by a negative linear relationship. The simulated scenarios indicated decreases in both recharge volumes and the hydraulic head coincided with increases in rainfall intensities, while recharge rates and runoff of groundwater increased with modest intensities (≤75 mm/h) increasing and decreased when intensities became larger (>75 mm/h). Though recharge rate and runoff for different rainfall intensities did not approach a common value, but instead stabilized at different values for each rainfall intensity event. It was concluded that rainfall intensity has great influence on groundwater regime. These are of great importance in ecological basic flow protection, river harnessing and watershed management in some extent.

1. Introduction

The dynamic changes of climate and human activities have altered the natural flow of rivers (Gadeke et al., 2014; Li et al., 2014; Richter et al., 1997; Sparks, 1992; Xu et al., 2014) and in some arid and semiarid regions, flow of many rivers continue to decrease, even appeared zero flow in dry season (Liu and Chen, 2000; Ren et al., 2002; Wang et al., 2006). Weihe River, located in the arid and semiarid regions of China, is a typical water deficiency and ecological basic flow shortage river, which has brought a great impact to the economic and social development of the region (Lin and Li, 2010; Liu and Hu, 2006). The amount of water infiltrating the soil surface directly affects the quantity of surface runoff and the recharge of both soil and ground water (Liu et al., 2011) which are the main sources of river flow. So the river flow, especially the ecological basic flow which maintained by groundwater during periods of low or no rainfall is affected directly by rainfall infiltration.

The quantity of surface runoff and soil recharge that came from rainfall is highly dependent on rainfall intensity and the relationships between them have been studied in detail (Huang et al., 2012; Jungerius and Ten Harkel, 1994; Schindewolf and Schmidt, 2012; Shigaki et al., 2007). By using a rainfall simulator, an experiment that was conducted in Loess Hilly region showed that rainfall intensity had significant effects on the runoff, and there was a negative exponential relationship between rainfall intensity and runoff coefficient (Li et al., 2014; Li and Huang, 2009; Li and Shao, 2004). The run off–on–out (ROOO) method was used to quantitatively measure the clay loam soil infiltrability under three rainfall intensities (20, 40 and 60 mm/h) and concluded that lower rainfall intensity resulted in higher infiltration rates and greater cumulative infiltration (Liu et al., 2011). Some workers claimed that rainfall intensities had a negative influence on infiltration because raindrop impact destroyed the surface aggregates of soils and gradually formed a continuous crust (Brandt and Thornes, 1987; Dunne and Leopold, 1978; Hoogmoed and Stroosnijder, 1984; Morin and Benyamini, 1977), which has very low hydraulic conductivity. Huang et al. (2012) conducted a quantitative study on soil infiltration and its factors using simulated outdoor rainfall events and found the recharge coefficient decreased with increasing of rainfall intensity.

* Corresponding author at: Institute of Soil and Water Conservation, Chinese Academy of Sciences and Ministry of Water Resources, Yangling, Shaanxi Province, China. Tel./fax: +86 29 87012066.
E-mail address: gaojianen@126.com (J.E. Gao).

http://dx.doi.org/10.1016/j.catena.2014.12.014
0341-8162/

And the covering measures that improve the relationship between rainfall intensity and soil infiltration also have been discussed extensively. For example, when the experiments were conducted under rangeland vegetation–soil associations (the soil was covered with rock, litter, vegetation base, grass, shrub, forb), the results from 19 rainfall simulation runs showed that the increase in infiltration rate with rainfall intensity increased from 0 to 176 mm/h (Stone et al., 2008). These covering measures dispersed the large raindrops into small raindrops, which reduced the actual rainfall intensity on the ground and made the rainfall intensity less than the infiltration capacity.

However, there is a need for more detailed investigations of rainfall intensity effects on groundwater recharge. Recharge results from effective precipitation (that is, precipitation minus losses from evapotranspiration) which infiltrate into the subsurface from where hydraulic gradients are downward (Taylor et al., 2013a). In many environments, natural groundwater discharges sustain baseflow to rivers, lakes and wetlands during periods of low or no rainfall (Taylor et al., 2013b), so increased attention was given to the effect of rainfall on groundwater recharge (Assouline and Mualem, 1997; Foley and Silburn, 2002; Hawke et al., 2006). However the impact of changing rainfall intensities on groundwater recharge remained unclear. Dourte et al. (2012) found that greater intensity storms might reduce groundwater recharge and increase runoff. However, Owor et al. (2009) using a rare set of coincidental observations of daily rainfall and groundwater levels in a seasonally humid equatorial basin (Upper Nile) found that projected increases in rainfall intensities as a result of global warming might promote rather than restrict groundwater recharge. In East Africa, Taylor and Howard (1996) found that rainfall and recharge had a nonlinear relationship and groundwater resources depended on extreme rainfall. Groundwater discharges sustain baseflow of Weihe River, so correctly estimating the groundwater recharge process over time is of importance for Weihe River in ecological basic flow protection, river harnessing and watershed management.

Both monitoring and modeling approaches have been used to measure or estimate groundwater recharge in the literatures. The monitoring approaches could be divided into physical methods and chemical methods (Sophocleous, 1993). The physical methods were (1) hydrometeorologic and soil–crop data processing to determine the soil–water balance or hydrologic balance of an area; (2) hydrologic data interpretation, including water table fluctuation analysis and different streamflow or streamflow separation (baseflow) analysis; and (3) soil–physics-based analysis, including estimation of water fluxes beneath the root zone using unsaturated hydraulic conductivity functions and the gradients in water potential, the zero-flux plane method, and lysimetry; the chemical methods included chemical and isotopic analyses of pore fluids from the saturated and unsaturated zones, with the results significantly affected by the mechanisms of infiltration. Because the monitoring approaches were very highly site-specific, expensive and time demanding, modeling approaches had become a trend and provided estimates of recharge rates over large areas. Fully saturated models, such as a three-dimensional finite-difference groundwater flow model, MODFLOW, were very popular and commonly applied to groundwater recharge problems (Jyrkama et al., 2002). A methodology was developed for linking climate models and MODFLOW to investigate future impacts of climate change on groundwater resources (Scibek and Allen, 2006). Zhang and Hiscock (2010) applied a groundwater flow model (MODFLOW) with a soil moisture balance recharge model to predict the effect of land-use change to forestry on groundwater recharge and levels in Nottinghamshire. Cho et al. (2009) used MODFLOW to determine the impact of land development activities on the subsurface flow regime in the Upper Roanoke River Watershed (URRW). The model interaction between surface water and groundwater also has become a trend, such as an integrated SWAT–MODFLOW was capable of simulating a spatio-temporal distribution of groundwater recharge rates, aquifer evapotranspiration and groundwater levels (Kim et al., 2008). But the accuracy of modeling results depended greatly on the accuracy of the information and the magnitude and distribution of the aquifer permeability (Sanford, 2002).

This paper combined monitoring method with modeling approach to estimate the effects of rainfall intensities on groundwater regime and it could provide a thought for ecological basic flow protection, river harnessing and watershed management.

2. Materials and methods

2.1. Simulated rainfall experiments

2.1.1. Experimental conditions and equipment

The simulated rainfall experiments were carried out in the Rainfall Simulation Hall of the State Key Laboratory of Soil Erosion and Dry land Farming on the Loess Plateau in Yangling District, Shaanxi Province, China. The simulated rainfall system has automatic simulation device of under sprinkler and the mean height of fall is about 18 m. The experiments were conducted in the soil box model (Fig. 1), 5.3 m × 1 m × 1 m at the Rainfall Simulation Hall (Wang et al., 2014). It was fitted with a jack to allow the slope to be adjusted from 0° to 35°. On the left and right of the model, there were two water tanks, 0.15 m × 1 m × 1 m, for the regulation of the groundwater level. Above the water tank, on the right there was one surface water groove and one drainage pipe of

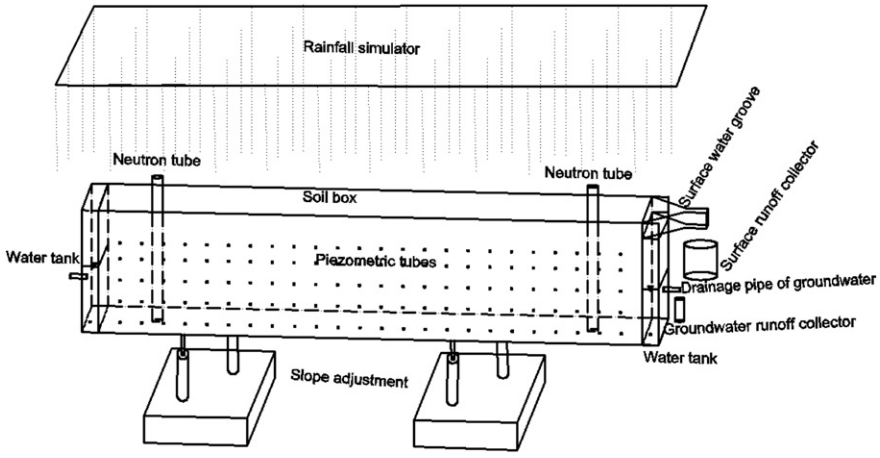

Fig. 1. The experimental flume.

groundwater at 0.39 m high. At the front side, one hundred and twenty sets of piezometric tubes were installed to observe the groundwater level. And two neutron probes were fixed in experimental flume for soil moisture control (Wang et al., 2013).

The size distribution and kinetic energy of raindrops are important factors in affecting rainfall infiltration and groundwater recharge (Eigel and Moore, 1983a, 1983b; Kinnell, 1981; Van Dijk et al., 2002; Wischmeier and Smith, 1958). The stain method (Cerdà et al., 1997; Eigel and Moore, 1983a; Shu et al., 2006) was used to measure raindrop size and distribution in this study.

The φ15 cm qualitative filter paper, which was produced in Xinhua Paper Mill of Hangzhou, Zhejiang Province, China, was selected as the absorbent surfaces and the eosin, which was produced in Dengfeng Chemical Reagent Factory of Tianjin, was selected as water soluble dye. Before rainfall experiment, the eosin was brushed on the filter paper evenly and the paper turned up resented pale pink, then the paper where was hit by raindrop would form a nearly circular red stain, just as Fig. 2.

The CorelDRAW software was used to measure horizontal and longitudinal diameters of stains with crossing method (Fig. 2). Then took the average value of horizontal and longitudinal diameters as stain diameter to calculate the raindrop diameter based on the equation (Eq. (1)) between drop size and stain size (Shu et al., 2006).

$$d = 0.36D^{0.73} \tag{1}$$

where d is the raindrop diameter (mm), and D is the stain diameter (mm).

Based on the relationship between accumulated volumes and raindrop diameters (Fig. 3), the raindrop median diameters ($d50$), which reflected the raindrop size distribution, were analyzed for different rainfall intensities.

The raindrop was an approximate sphere, so the total kinetic energy of filter paper can be calculated by the formula as follows.

$$e = \sum_{l}^{i} e_i = \sum_{l}^{i} \frac{1}{2} m_i v_i^2 = \frac{1}{2} \sum_{l}^{i} \pi d_i^3 \rho v_i^2 \tag{2}$$

where e is the total kinetic energy of filter paper (J), i is the i-th raindrop, e_i is the kinetic energy of the raindrop (J), m_i is the quality of the raindrop (J), v_i is the velocity of the raindrop (m/s), d_i is the raindrop diameter (mm), and ρ is the density of water (g/cm^3).

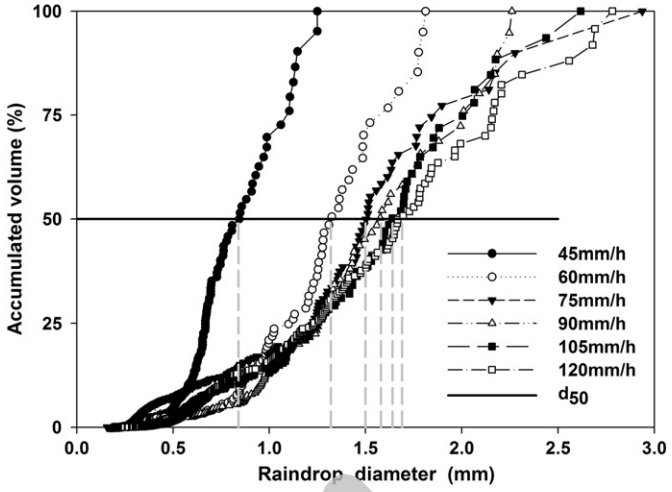

Fig. 3. The relationship between accumulated volume and raindrop diameter.

Based on the total kinetic energy of filter paper (e), every millimeter rainfall raindrop kinetic in unit area could be calculated through a formula as follows.

$$E = \left(\frac{e}{S}\right) \Big/ \left(\frac{M}{\rho S}\right) = \frac{e\rho}{M} = \frac{e\rho}{\sum_{l}^{i} m_i} = \frac{e\rho}{\sum_{l}^{i} \frac{1}{6}\pi d_i^3 \rho} = \frac{e}{\sum_{l}^{i} \frac{1}{6}\pi d_i^3} \tag{3}$$

where E is the raindrop kinetic of every millimeter rainfall in unit area (J/m^2/mm), S is the area of filter paper (m^2).

Different formulas were used to calculate the raindrop fall velocities according to raindrop sizes. When the raindrop diameter was less than 1.9 mm, the improved Sha Yuqing formula was selected to calculate the velocity.

$$v = 0.496 \times 10^{\left[\sqrt{28.32 + 6.524 lg0.1d - (lg0.1d)^2} - 3.665\right]} \tag{4}$$

when raindrop diameter was not less than 1.9 mm, the raindrop fall velocity was calculated by the improved Newton formula.

$$v = (17.20 - 0.844d)\sqrt{0.1d} \tag{5}$$

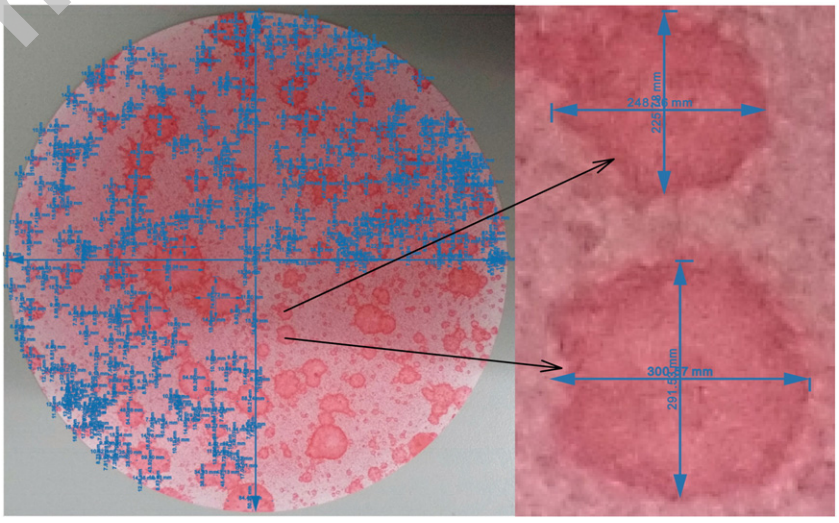

Fig. 2. Base on crossing method to measure stain diameters (120 mm/h).

where v is the fall velocity of raindrop (m/s). Table 1 showed the simulated rainfall experiment conditions and the results of E under different rainfall intensities.

2.1.2. Experimental materials and treatment

The test materials included riversand and Lou soil. The riversand samples were dug from the middle and lower reaches of the Wei River bank in Yangling District and the Lou soil was also collected from Yangling District, Shaanxi Province, China (Wang et al., 2013). And the soil samples were air-dried for about ten days and sieved through a series of corresponding magnitude sieves. Then they were packed into the flume layer by layer from bottom to top as Fig. 4. The top layer was about 0.5 cm thick and filled with the composite sandy loam. The mixed soil was composed of riversand and Lou soil. The weight ratio of this composite soil was about 2:5 and its average soil bulk density was about 1.6 g/cm^3. The middle layer, filled with the fine sand, was about 1 cm thick and its average soil bulk density was also about 1.6 g/cm^3. The bottom layer, filled with the medium sand, was about 98.5 cm thick and its average soil bulk density was about 1.4–1.5 g/cm^3. From Fig. 4, we also could see the mechanical composition of every soil layer.

The experimental flume was fixed at an angle of 3° in this study. Six gradient rainfall intensities (45/60/75/90/105/120 mm/h) with uniform rainfall conditions were simulated correspondingly and the precipitation for a control to be equal was 120 mm. The main monitoring items measured during the experiments were: the surface runoff amount, the surface runoff in the process, groundwater flow, groundwater level, soil moisture and water temperature.

2.2. Visual MODFLOW

The software used for this study was Visual MODFLOW, which integrates MODFLOW, MODPATH, MT3DMS, WinPEST, Zone Budget, and other modules. It also supports both the calibration and predictive analysis capabilities of the PEST-ASP program, and it allows you to run parameter estimation using results from both groundwater flow and contaminant transport simulations (Hydrogeologic, 2005).

Based on the simulated rainfall experiments, the conceptual model was established first. The model was divided into a 50 × 265 array of 4×10^{-4} square meter cells uniformly. It consisted of three individual layers with a gradient of 3° and the thicknesses were 0.5, 1 and 98.5 cm respectively from top to bottom. The flow type was transient flow and the time unit was minute. The edges of the model acted as no-flow boundaries. The calculation of groundwater recharge was executed on a minute with input data of rainfall. The drainage pipe of groundwater was treated as a flux boundary in the form of a pumping well. Observed hydraulic heads from monitoring system were used to compare with the simulation results. And the flow model requires conductivity, storage, and initial head property values for each active grid cell in order to run a flow simulation (Hydrogeologic, 2005).

3. Results and discussion

3.1. Parameter calibration of Visual MODFLOW model

The main parameters of the model were: recharge coefficient (Rc), hydraulic conductivity (Kx, Ky, and Kz), storage (specific storage (Ss), and specific yield (Sy)). Initially, based on the simulated rainfall experiment of 75 mm/h rainfall intensity, the model was calibrated manually for the initial set of parameters and subsequently the values of parameters were adjusted accurately using PEST during the optimization process. Calibrated MODFLOW parameters were shown in Table 2.

The scatter graph during the whole period and the typical period (t = 120 min) of the calibration in Fig. 5(a) and (b) showed that most of the data points intersect the 1:1 line on the graph. Meanwhile the calibration statistics were showed in Table 2, including the residual mean (RM), the absolute residual mean (ARM), the standard error of the estimate (SEE), the root mean squared error (RMS), the normalized root mean squared (NRMS) and the correlation coefficients (Cor) for groundwater heads of 48 piezometric tubes on the bottom two rows of tubes during the whole simulation period.

Then the mass balance which was one of the key indicators of a successful simulation (Hydrogeologic, 2005) was analyzed. The flow mass balance graph (Fig. 6) showed the volume of water entering and leaving the system through the flow boundary conditions, and from aquifer storage at the end of the simulation period. The total volume flow into this entire system was 0.2720 m^3 which included 0.0644 m^3 storage and 0.2076 m^3 recharge. The total volume flow out of this model was 0.2718 m^3 which consisted of 0.1345 m^3 storage and 0.1373 m^3 well. The mass balance error for the simulation inflow and outflow was 0.22%. Since the model has been adequately calibrated based on the simulated rainfall experiment, the results of the calibration in groundwater balance, levels can generally be considered acceptable (Hydrogeologic, 2005).

Results of calibration statistics and flow mass balance were all within the allowable range, so the model was calibrated. Thus, it was applied to studying the influence of different rainfall intensities on groundwater recharge, flow and levels.

3.2. Recharge coefficients for different rainfall intensities based on parameter inversion

After calibration of the model, Visual MODFLOW models for rainfall intensities 45/60/90/105/120 mm/h were simulated. Fig. 7 was the scatter graph of calculated vs. observed values. We could see whether the simulations for rainfall intensities 45/90 mm/h during the typical period (Fig. 7(a), (b)) or the scatter graph for rainfall intensities 105/120 mm/h during the whole simulation period (Fig. 7(c), (d)) showed the data points deviated from the X = Y line, so the calculated heads could not characterize the observed values well. These results indicated that rainfall intensity had a great impact on the changes of groundwater level. And recharge coefficient was the only parameter related to rainfall intensity directly in this model.

Table 1
Simulated rainfall experiment conditions under different rainfall intensity.

No.	I mm/h	Nozzle combination	Pressure (Kp)	Uniformity (%)	$\bar{I}$ mm/h	$d50$ mm	E J/m^2/mm
1	45	1	k = 75	87.02	46.44	0.84	6.05
2	60	2	k = 90	89.02	54.53	1.32	13.22
3	75	2	k = 120	91.53	79.95	1.5	16.37
4	90	1, 3	k = 25	91.61	92.56	1.58	16.97
5	105	1, 3	k = 48	85.13	113.35	1.64	17.5
6	120	1, 3	k = 55	84.75	126.7	1.69	18.18

Where I is the calibrated rainfall intensity, $\bar{I}$ is the average rainfall intensity during rainfall.

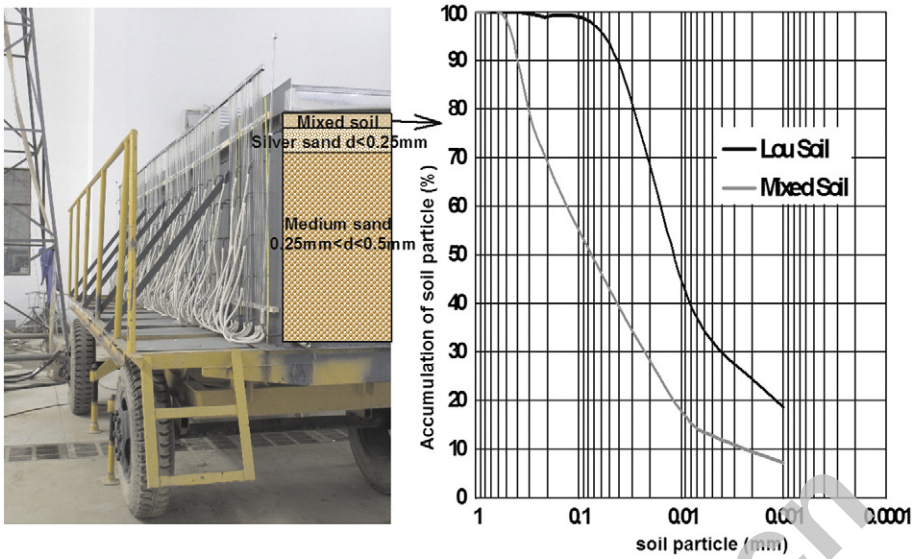

Fig. 4. The test tank filling and mechanical composition of soil.

So recharge coefficients for different rainfall intensities were calculated by using parameter inversion method based upon the PEST-ASP program of Visual MODFLOW combined together with the parameter regulating manually. And the more ideal parameters of recharge coefficients were 0.439, 0.345, 0.167, 0.138 and 0.076 for rainfall intensities 45/60/90/105/120 mm/h respectively. Fig. 8 was the corresponding scatter graph of calculated vs. observed values and showed that most of the data points intersect the 45 degree line on the graph during the whole simulation period (Fig. 8(a), (b), (c)) and at the typical period (t = 120 min) (Fig. 8(d), (e)). Furthermore, the statistical results were analyzed in Table 3. It indicated that all error indicators were within the allowable range. So the simulated groundwater levels matched the observed heads well.

To verify the simulated groundwater recharge further, water balances including rainfall, surface water, soil water and groundwater for six rainfall intensities were calculated based on the simulated rainfall experiments. The total rainfall was 0.599 m^3 for all experiments; runoff and accumulated volume processes of surface water were showed in Fig. 9. So we could get a corresponding process of infiltration. The soil moisture was tested before and after every experiment by neutron probes fixed in an experimental flume. The average increases in soil moisture for six rainfall intensity scenarios increased from 0.060 to 0.087 m^3 with a mean value of 0.070 m^3 (Fig. 10). It was apparent that there were only modest differences between the different scenarios in terms of the average increase in soil moisture for the whole layer. Hence, comparison results between calculated groundwater recharge based on water balances and simulated recharge based on MODFLOW could be analyzed (Fig. 10). The error range for six rainfall intensity scenarios was −4.78%–5.69%. Results of the simulation may generally be considered acceptable, provided the observational errors during the experiments and the systematic bias of simulation results.

In order to compare the influence of rainfall intensities on recharge coefficients quantitatively, regression analyses were conducted (Fig. 11), yielding the relationship between them in Eq. (7).

$$Rc = -0.0049I + 0.6566 \quad (7)$$

where *Rc* and *I* denote the recharge coefficient (%) and rainfall intensity (mm/h), respectively. The model's correlation coefficient, R = 0.979, F = 93.95, and P = 0.006 indicated that it had a high predictive capability.

The recharge coefficient decreased linearly with the increase of the rainfall intensities. From Table 1, we could see that with the simulated rainfall intensity increasing, both the median diameter and rainfall raindrop kinetic increased. Increasing the rainfall intensity yielded raindrops with more kinetic energy (Salles et al., 2002; Winder and Paulson, 2012), which would destroy the structure of the near-surface soil structure (Hawke et al., 2006; Huang et al., 2012; Joel and Messing, 2001; Liu et al., 2011) in a number of ways: the compressive forces might destroy or deform the particle arrangement, the shear forces may dislodge or disrupt the orientation and position of surface particles or aggregates, aggregates might disintegrate due to slaking, and the pores might become clogged with detached particles as the rainfall infiltrates (Romkens et al., 1986). The hydrological response of the soil was controlled by successive changes in the properties of the surface soil (Bowyer-Bower, 1993) and raindrop impact destroyed the surface aggregates of soils and gradually formed a continuous sealing and crusting (Morin and Benyamini, 1977) by flowing water which gave the soil surface a has very low hydraulic conductivity (Stroosnijder and Hoogmoed, 1984). The soil surface became less than the permeability of the soil beneath the surface, and limits the rate at which water could enter the soil (Bowyer-Bower, 1993; Li and Shao, 2004; Schmidt, 2010). Result indicated that the skin seal (crust) had 2000 times lower permeability than the underlying soil layers (McIntyre, 1958). Romkens et al. (1986) reported that seal development was apparently affected by rainfall intensity, but gave no physical explanation for this response. Results of simulated rainfall experiments on surface runoff & volume vs. rainfall intensities (Fig. 9) further confirmed that increases in rainfall intensities might reduce groundwater recharge and increase runoff, making the surface storage of runoff increasingly important to enhance recharge and reduce flooding risks (Dourte et al., 2012b; Huang et al., 2012; Wischmerie and Smith, 1979).

When rainfall intensities increased from 45 mm/h to 120 mm/h, the recharge coefficients decreased from 0.439 to 0.076 with a mean value

Table 2
The main calibrated parameters of the MODFLOW model.

Parameters	*Rc*	Kx1(m/s)	Kz1(m/s)	Kx2(m/s)	Kz2(m/s)	Kx3(m/s)	Kz3(m/s)	Sy	Ss
Calibrated value	0.327	1.12×10^{-7}	2.52×10^{-9}	1.50×10^{-6}	7.47×10^{-7}	3.1×10^{-4}	7.60×10^{-5}	0.36	1.385×10^{-4}

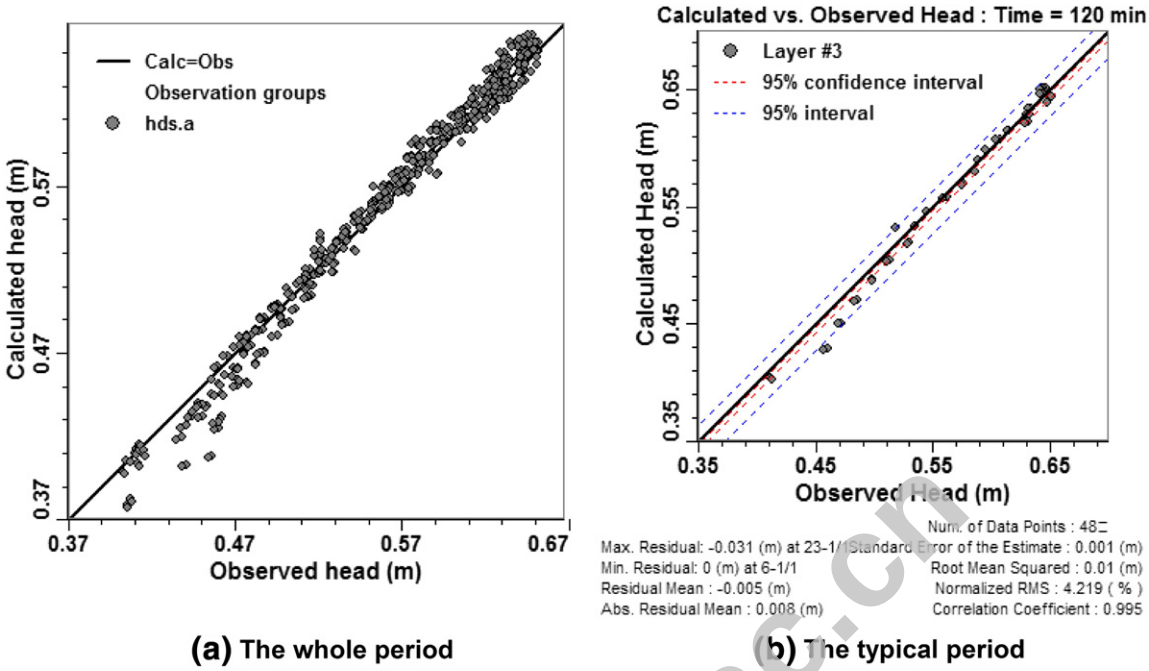

Fig. 5. The scatter graph of calculated vs. observed values.

of 0.249. Compared to results of simulated rainfall experiments, the mean recharge coefficient was slightly smaller than the result (0.28) conducted by Feng et al. (1998) and much smaller than the mean value (0.549) from Huang et al. (2012), while it was larger than the average recharge coefficient (0.145) studied under the natural rainfall (Table 4). Table 4 reviewed many studies about recharge coefficient using models, tracers and conventional methods in various hydrological environs, and we could see that the range from 0.012 to 0.526 was similar to the range of this study. Each of these values might be apt for the environment in which they were observed, however, the phenomenon appeared quite widespread, across many soil types and rainfall conditions, suggesting that a more inclusive mechanism might be responsible (Foley and Silburn, 2002).

Although there was a high negative linear correlation between recharge coefficients and rainfall intensities, the relationship was not perfect. When rainfall intensity increased from 75 mm/h to 90 mm/h, recharge coefficient decreased sharply. Some studies also found that there was an inflection around 80 mm/h for the research on rainfall infiltration (Hawke et al., 2006; Li and Shao, 2004; Merz et al., 2002). Hawke et al. (2006) and Li and Shao (2004) investigated the influence of rainfall intensity and initial soil water content on changes in hydraulic conductivity and found that when rainfall intensity increased towards 80 mm/h the smooth relationship of soil water potential began to breakdown. They also found that this breakdown was not observed at any other rainfall intensity and probably coincided with textural disruption of the soil. Merz et al. (2002) represented the mean dependency between final infiltration rate and rainfall intensity and they also found that the curve for rainfall intensities larger than 80 mm/h was very much influenced by only one experiment and has no explanation power.

3.3. The relationship between recharge rate and rainfall intensity

All time-series lines of infiltration rate with rainfall intensities exhibited similar trends (Fig. 12) that the infiltration rate initially decreased sharply at the beginning of rainfall then decreased gradually at a stabilized value. It was attributed to the initial infiltration that the capacity of a dry soil was high, as rainfall continued, and as the soil became saturated, it diminished to a relatively constant rate (ultimate capacity) (Horton, 1919). According to the time-series infiltration and

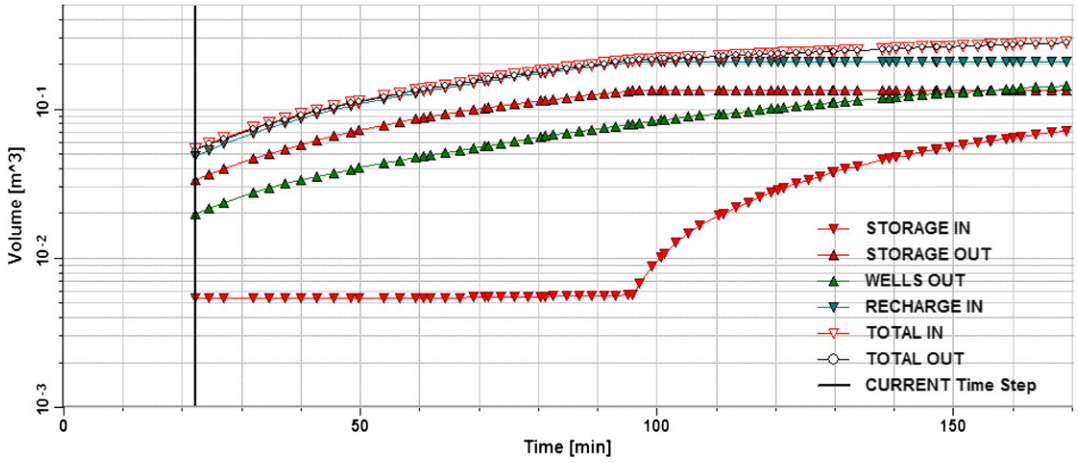

Fig. 6. The calculation temporal flows IN and OUT of the system.

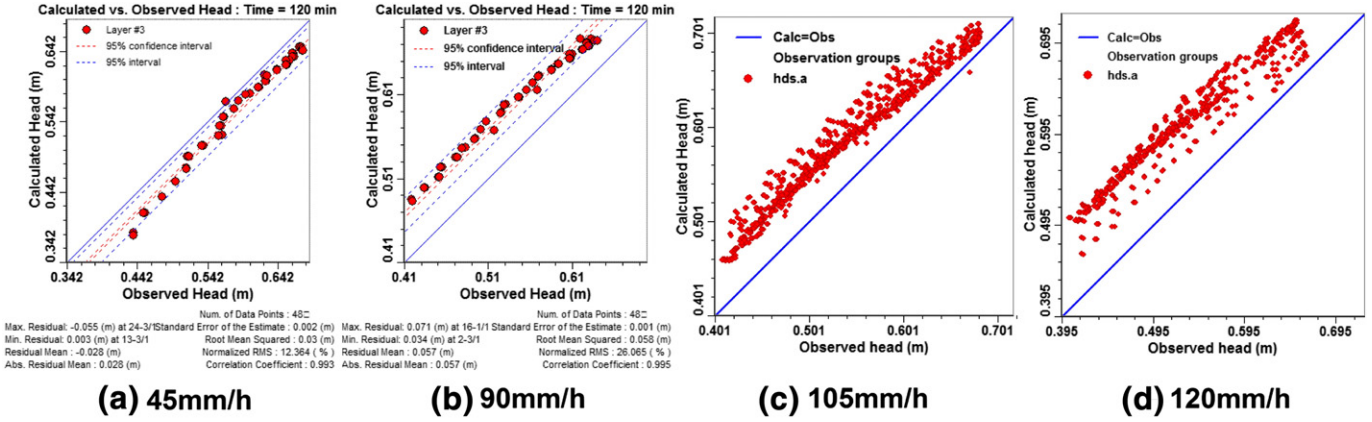

Fig. 7. The scatter graph of calculated vs. observed values based on the calibrated parameters.

groundwater flow, the processes of groundwater recharge rate during the whole rainfall experiment were calculated for different rainfall intensities. And the average recharge rate of one test increased by 1.4 times with rainfall intensity increased from 45 mm/h to 75 mm/h, however, for situations of 75/90/105/120 mm/h rainfall intensities, it decreased by approximately a factor of 2.6 with increasing rainfall intensity. The mean recharge rates also increased with low intensity rainfall ($I \leq 75$ mm/h) increase and decreased with high intensity ($I \geq 75$ mm/h) increase (Fig. 13). Just as was said by Horton (1919), when the rainfall intensity was less than the infiltration capacity, all of the water reaching the ground could infiltrate. But if the rainfall intensity exceeded the infiltration capacity, infiltration would occur only at the infiltration capacity rate, and water in excess of that capacity would be stored in depressions, became surface runoff, or evaporated.

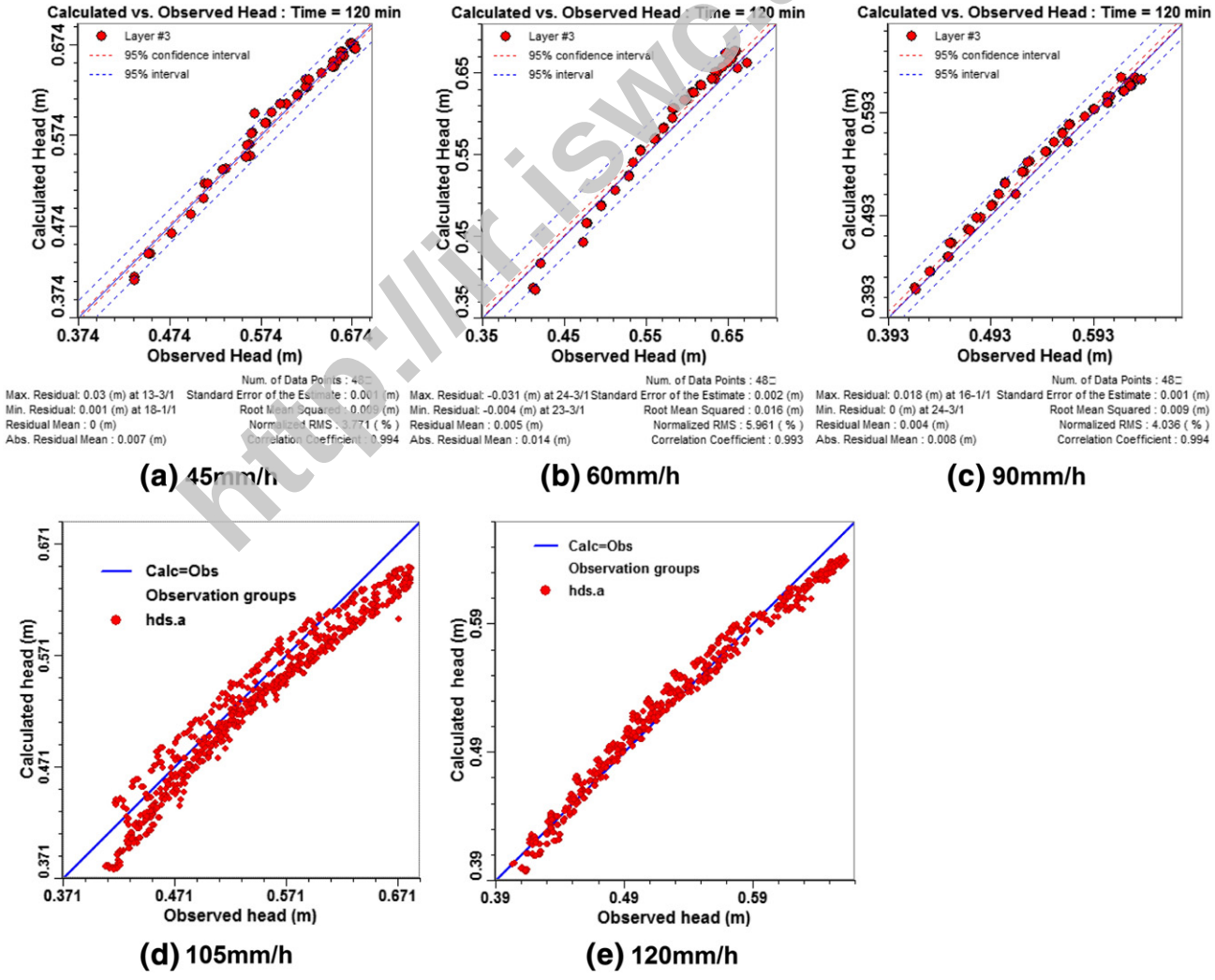

Fig. 8. The scatter graph of calculated vs. observed values. These results were obtained on the premise of the other parameters and of the same recharge coefficient calibrated for different rainfall intensities.

Table 3
Error indexes of calculated vs. observed values under different rainfall intensities.

Evaluation indexes	RM (m)	ARM (m)	SEE (m)	RMS (m)	NRMS (%)	Cor
Calibration (75 mm/h)	0.0002	0.00727	0.0012	0.0097	4.146	0.996
45 mm/h	0.000375	0.00843	0.00119	0.00981	4.259	0.994
60 mm/h	−0.0032	0.0148	0.0020	0.0181	7.861	0.992
90 mm/h	−0.0019	0.0130	0.0015	0.0148	6.490	0.994
105 mm/h	0.0006	0.0126	0.0017	0.0146	6.510	0.993
120 mm/h	0.0008	0.0088	0.0015	0.0105	5.375	0.993

Though rates for different rainfall intensities did not approach a common value, but instead stabilized at different values for each rainfall intensity event.

Regression analyses were conducted to study the relationship between rainfall intensity (I, mm/h) and the mean recharge rate (MRR, cm/min) (Fig. 13). The average recharge rate varied with rainfall intensity following a parabolic function law (Eq. (8)).

$$MRR = -6.857 \times 10^{-6} I^2 + 0.0009I + 0.0109. \quad (8)$$

3.4. The relationship between groundwater flow and rainfall intensity

The total volume flow out of the model consisted of storage out and well out. The graph in Fig. 14 showed changes of total groundwater flow for six different rainfall intensities of a given total rainfall (approx. 120 mm). It was clear that the relationship between rainfall intensity and the groundwater flow was complex. Noticeable trends that the discharge increased with low intensity rainfall ($I \leq 75$ mm/h) increase and decreased with high intensity ($I \geq 75$ mm/h) increase were observed. Owing to the fact that infiltration rate was limited to the rainfall intensity, when rainfall intensity was higher than the soil infiltrability, excess rainwater began to pond on the soil surface and then to run off as overland flow (Liu et al., 2011). Though there were significant differences in high or low flow rate of groundwater among different rainfall scenarios, all time-series graphs for six rainfall intensities exhibited similar trends.

Different from the trends of surface water runoff, which increased with rainfall intensity increasing (Fig. 9), for all scenarios, the groundwater flow initially decreased sharply first and then stabilize gradually with the passage of rainfall time. The increase of average flow for rainfall intensity of 75 mm/h was more than four times as large as that for rainfall intensity of 60 mm/h compared with the 45 mm/h event. When the rainfall intensity increased from 75 mm/h to 90 mm/h, the average flow decreased by 37.02%. Then with the rainfall intensity increased, the average discharge fell continually, even fell by 50.85%. Table 5 summarized the average runoff and change values of groundwater for six different rainfall intensities with a constant amount of rainfall.

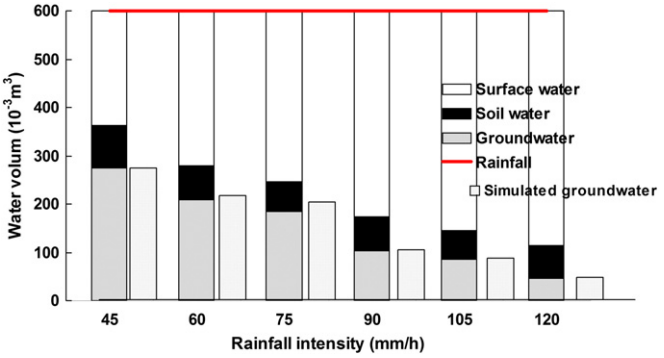

Fig. 10. Comparison results between the calculated recharge and the simulated recharge.

In a word, increases in rainfall intensity were not conducive to groundwater flow and might reduce the value for less infiltration. For modest intensities, increases in the intensity of the rainfall gave higher increase of flow. However, as the intensities became larger, this relationship reversed.

3.5. The relationship between groundwater level and the rainfall intensity

Groundwater level might be changed due to variation of recharge. Analyzed differences in the magnitude of groundwater level fluctuations arise from rainfall intensity variations (Table 6, Figs. 15 and 16). After the termination of the rainfall, the average level across the entire profile of 45 mm/h rainfall intensity event increased by approximately a factor of 11.7%, to a maximum possible change value of 6.29 cm compared to initial head of simulations. The average levels of 60 mm/h and 75 mm/h events increased somewhat less, while increases for the average level under 90–120 mm/h simulations were less than a factor of 5%. The faster response of higher rainfall intensity conditions was attributed to the greater energy imparted to the soil surface per unit time; this altered the properties of the soil surface more quickly than the lower energy per unit time of lower rainfall intensities (Bowyer-Bower, 1993).

Contrastingly, at the 160 min following the termination of the longest rainfall duration scene (45 mm/h), groundwater levels for different rainfall intensities showed a different trend (Fig. 15, Table 6). Flow field of groundwater at 160 min for different rainfall intensities were presented in Fig. 15. Table 6 showed that groundwater levels responded to the changes in groundwater recharge for rainfall intensity variations. Before termination of the 45 mm/h rainfall event, other 5

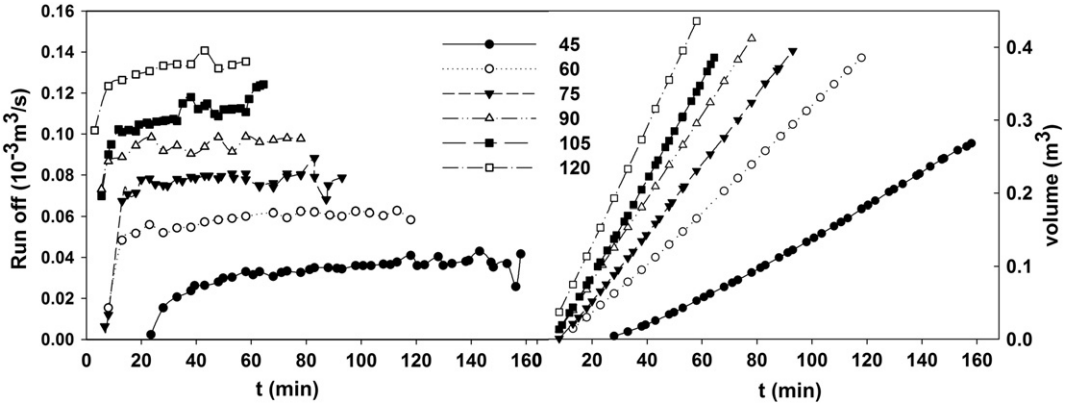

Fig. 9. Time-series graphs of the surface runoff and accumulated water volume.

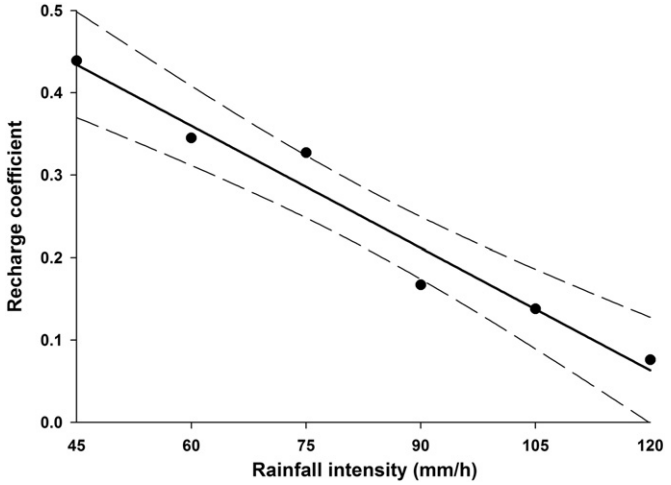

Fig. 11. The relationship between the recharge coefficient (*Rc*) and the rainfall intensity (*I*).

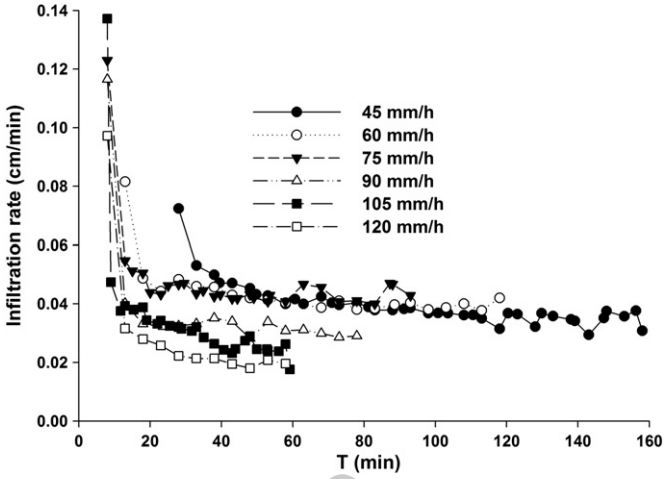

Fig. 12. Time-series infiltration rate for six rainfall intensities.

rainfall intensity events had successively finished since t = 60 min, so no water supplies were continually provided, groundwater level would gradually decrease due to the groundwater flow. The average value and change of groundwater level at t = 160 min shown in Table 6 did show a large variation in groundwater levels compared with the earlier results where the simulations were analyzed after the termination of the rainfall recharge values. The average groundwater levels across the entire profile for 60 and 75 mm/h rainfall intensities increased 3.44 cm and 0.71 cm compared with the initial head, while that for bigger intensities (>75 mm/h) decreased sharply, even smaller than the initial head. Overall, falls in groundwater level were found in response to a reduction in recharge.

Comprehensive analysis of average groundwater levels at 48 observed wells during the 0–160 min period showed noticeable trends of increasing along the position of experimental transect for all rainfall intensities events, but there were significant differences in the amplitude of groundwater level increases among different events (Fig. 16, Table 6). In the space domain, the levels increased for almost all sites, except for a few sites at the end of transect (about >4 m) with larger rainfall intensities ($I \geq 75$ mm/h). The largest changes in mean groundwater level occurred in the 45 mm/h rainfall intensity scenario, increased from 0.04 cm to 6.23 cm with a mean value of 4.45 cm, increased by 8.27% compared with the initial head. The changes in groundwater level caused by rainfall intensities that changes in other scenarios account for less than 6% across the entire profile (Table 6). The larger levels obtained with lower rainfall intensities were attributed to the greater energy disrupting the sealing of the soil surface.

Furthermore, the measurements and modeling were executed under very specific conditions and did not consider the changes of complex underlying surface and aquifer characteristics. Therefore, the

Table 4
Recharge coefficient of literatures in various hydrological environs.

Literature	Site	Method	Recharge coefficient	
			Range	Average
Moreno and Vieux (2011)	Oklahoma	A rainfall–runoff model	0.052–0.369	0.198
Dourte et al. (2012)	Peninsular India	Rainfall IDF relationships	0.098/0.103	0.105
Wang et al. (2008)	Lu Quan	The ^{3}H, Br^{-} tracer method	0.188–0.244	0.213
	Luan Cheng		0.082–0.526	0.221
	Xin ji China		0.140–0.166	0.153
	Shen Zhou		0.139–0.219	0.179
	De Zhou		0.082–0.324	0.224
	Cang Zhou		0.114–0.175	0.143
Tan et al. (2013)	North China Plain	The Br^{-} tracer method	0.0532–0.396	0.185
Sukhija et al. (1996)	L.R. Palayam	The Cl^{-} tracer method	0.256	0.256
	Murattandi		0.155	0.155
	Idayanchavadi		0.134	0.134
Zhu et al. (2007)	Minqin Basin, Northwest China		0.0149	0.0149
Gates et al. (2011)	semi-arid Loess Plateau,China		0.11–0.18	0.098
Huang and Pang (2011)	Guyuan in the Loess Plateau of China		0.12	0.12
	Xifeng in the Loess Plateau of China		0.06	0.06
Sukhija and Shah (1976)	Pondicherry	The Cl^{-}, ^{3}H tracer method	0.235	0.235
Goel et al. (1975)	Western	The ^{3}H tracer method	0.217	0.217
	Punjab India		0.178	0.178
	Haryana		0.170	0.170
Sharma and Gupta (1985)	Western Rajasthan		0.056–0.135	0.097
Sukhija and Rama (1973)	Gujarat		0.03–0.109	0.055
Goel et al. (1975)	Northern India		0.17–0.22	0.19
Rangarajan et al. (1989)	Neyveli groundwater basin		0.134	0.134
Athavale et al. (1983)	Kukadi basin		0.075	0.075
	Godavari-Purna		0.086	0.086
Athavale and Rangarajan (1988)	Semi-arid India		0.012–0.133	0.062
Lin and Wei (2006)	Wudan county, Inner Mongolia Autonomous Region of China		0.13	0.13
	Pingding County, Shaanxi Province		0.12	0.12
Total			0.012–0.526	0.145

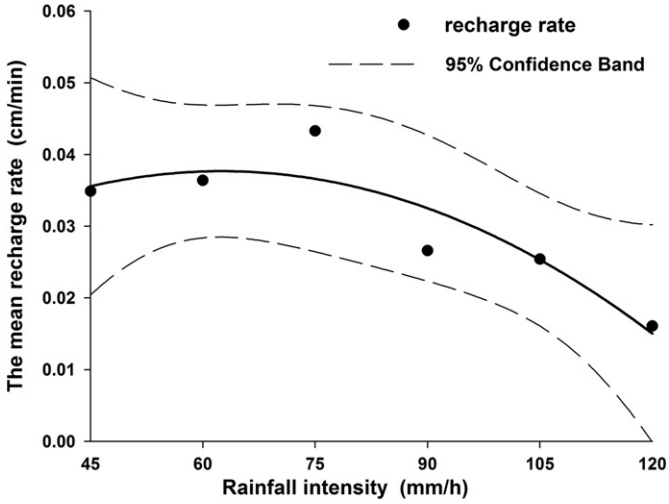

Fig. 13. The relationship between mean recharge rate (MRR) and rainfall intensity (*I*).

results of this study could not be compared directly with those from large-scale areas and it may be difficult to transfer these results to the field quantitatively (Hawke et al., 2006; Huang et al., 2012). However, since the rainfall simulation experiments were a widely used method in rainfall–runoff research and the modeling was calibrated well, the results may be used to qualitatively study the change laws in large scale areas. So this study was still helpful to improve the understanding of the effects of rainfall intensity on groundwater regime or it might provide a thought for studying at least.

4. Conclusions

Rainfall intensity, which is one of the most important characteristics of rainfall, has an effect on surface runoff and the recharge of both soil and ground water. So it affects the river flow directly, especially the ecological basic flow which is maintained by groundwater during periods of low or no rainfall. Based on the artificial rainfall experiments and groundwater model (Visual MODFLOW), the effects of rainfall intensity on groundwater regime were studied.

Groundwater recharge coefficients for six rainfall intensities with a constant amount of rainfall were calculated through iterative solution done many times and the results of scatter graph, calibration statistics and flow mass balance showed that the predicted results matched well with the observed data. Meanwhile the groundwater recharges

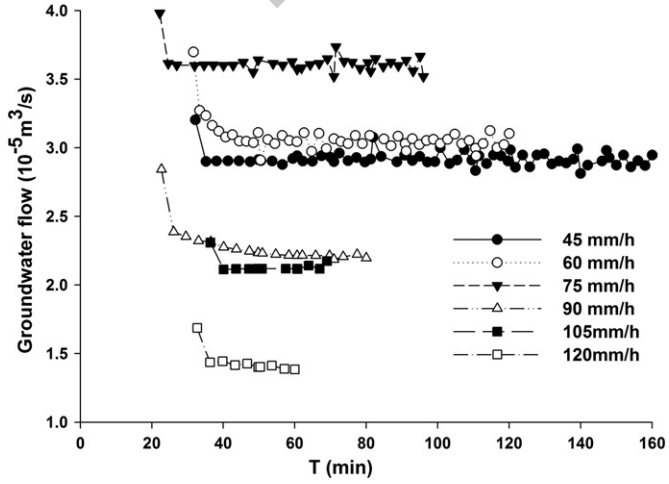

Fig. 14. Time-series analysis on groundwater flow for six different rainfall intensities.

Table 5
The average runoff flow and change value of groundwater for six different rainfall intensities.

Rainfall intensity (mm/h)	45	60	75	90	105	120
The average value (10^{-5} m^3/s)	2.93	3.05	3.62	2.28	2.14	1.44
Change (%)	0	4.10	23.55	−22.18	−22.96	−50.85

were also calculated based on water balances and the error range between the calculated recharge and the simulated recharge based on MODFLOW was acceptable. Recharge coefficients and rainfall intensity had a high negative linear correlation and recharge coefficients decreased from 0.439 to 0.076 with rainfall intensity increased from 45 mm/h to 120 mm/h. This negative correlation could be attributed to the positive relationship of intensity and raindrop kinetic. The larger rainfall intensity yielded raindrops with more kinetic energy which would destroy the surface aggregates of soils more serious and gradually formed a continuous sealing quicker. So under the bare slope condition, the heavier rainfall would produce less groundwater recharge and it would not be helpful to ecological basic flow protection.

The recharge rate increased with rainfall intensity increase from 45 mm/h to 75 mm/h, whereas that decreased gradually with increasing rainfall intensity from 75 mm/h to 120 mm/h. The recharge rates for different rainfall intensities did not approach a common value, but instead stabilized at different values for each rainfall intensity event. The results of groundwater flow simulations showed similar trends as those for the recharge rate, with reductions in recharge rate sometimes causing decreases in flow. The groundwater flow initially decreased sharply but then decreased gradually until to a stabilized value. When the rainfall intensity increased from 45 mm/h to 120 mm/h, the average groundwater flow increased initially and then fell gradually. The highest average runoff was achieved at a rainfall intensity of 75 mm/h. These results were consistent with the infiltration laws. When the rainfall intensity was less than the infiltration capacity, all of the rain water could infiltrate. As the intensity increases, if it exceeded the infiltration capacity, infiltration would occur only at the infiltration capacity rate.

Groundwater level changed due to variation of recharge. After the termination of the rainfall, the situation for 120 mm/h rainfall intensity had the lowest average level compared with the initial head of simulation. Then the average level increased with the rainfall intensity decreasing gradually. Contrastingly, after 160 min following the termination of the longest rainfall duration scene (45 mm/h), groundwater levels for different rainfall intensities showed that groundwater levels gradually decreased and responded to the changes in groundwater recharge for no water supplied continually. The average groundwater levels across the entire profile for 60–75 mm/h rainfall intensities increased 3.44 cm and 0.71 cm compared with those from the initial head, while that for bigger intensities (>75 mm/h) decreased sharply.

Although the results of this study are difficult to extrapolate to larger scales quantitatively for the relatively specific conditions, they are useful to understand the great influences of rainfall intensities on recharge volume, recharge rate, runoff and heads of groundwater. It

Table 6
The changes in groundwater level for six different rainfall intensities during different period.

Period	Level (cm)	Initial head	45 mm/h	60 mm/h	75 mm/h	90 mm/h	105 mm/h	120 mm/h
The end period of rainfall	Average	53.74	60.03	57.69	57.44	56.27	55.91	55.50
	Change	0	6.29	3.95	3.7	2.53	2.17	1.76
0–160 min	Average	53.74	58.19	56.97	56.07	55.32	54.98	54.52
	Change	0	4.45	3.22	2.33	1.58	1.23	0.78
T = 160 min	Average	53.74	60.03	57.18	54.45	52.85	51.83	51.54
	Change	0	6.29	3.44	0.71	−0.89	−1.91	−2.2

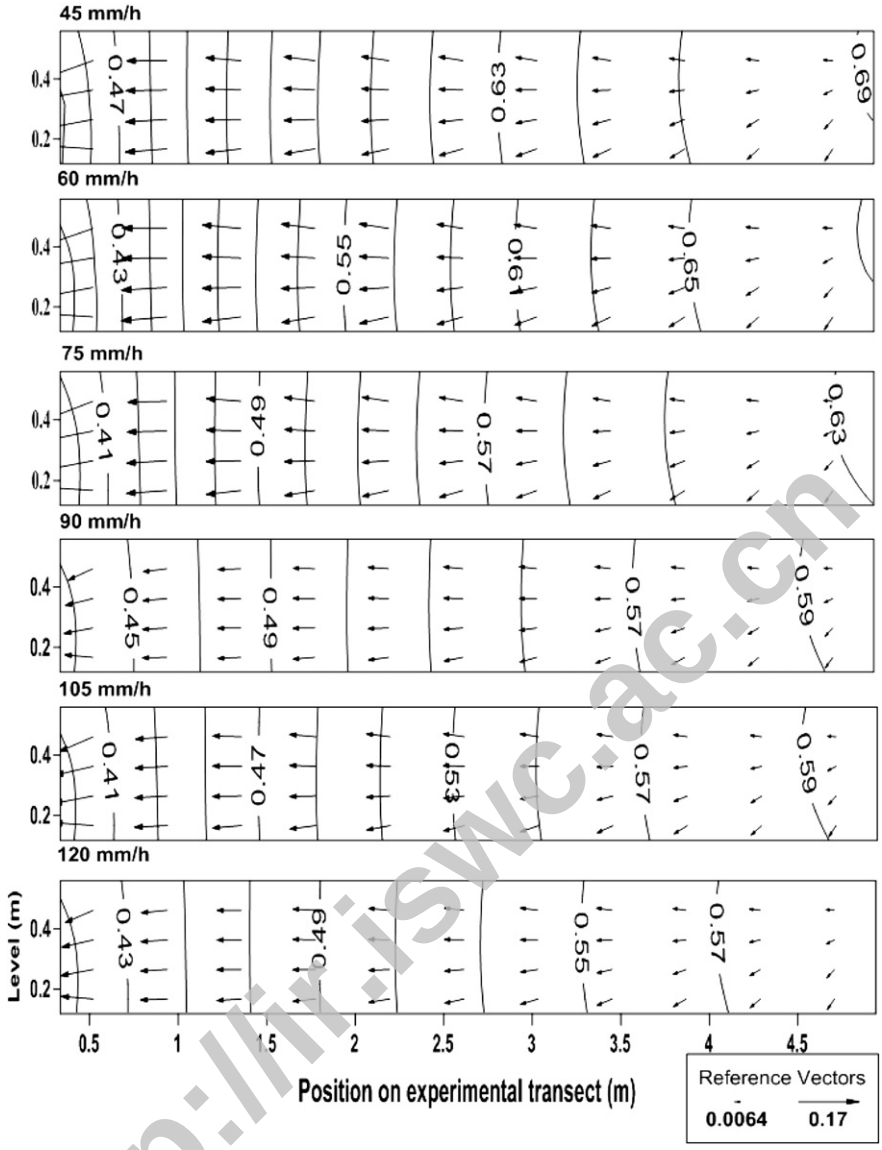

Fig. 15. Flow field of groundwater at 160 min for six different rainfall intensities (the direction of reference vectors stands for flow direction of groundwater and the size of reference vectors only means high or low velocity of flow, not the exact value of flow rate).

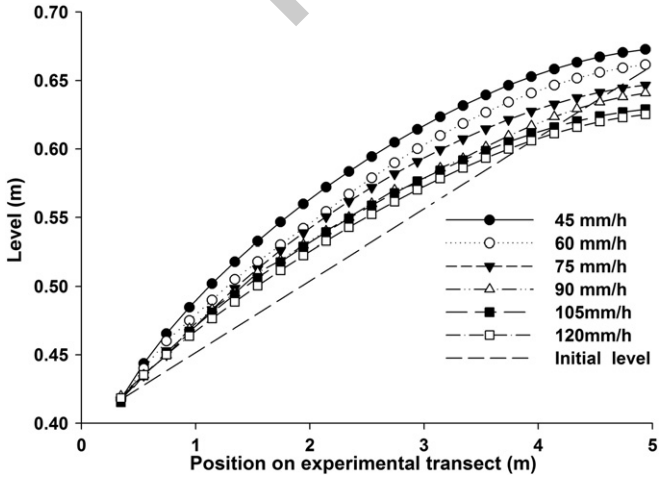

Fig. 16. The average groundwater levels at 48 observed wells during the 0–160 min along the position of experimental transect for six different rainfall intensities.

might provide support or a thought for ecological basic flow protection, river harnessing and watershed management in some extent.

Acknowledgments

This paper was supported by the Natural Science Foundation of China (41371276), by the National Technology Support Project (2011BAD31B05) by the Subject of the National Science and Technology Major Project (2009ZX07212-002-003-02), by Knowledge Innovation Project of Institute of Soil and Water Conservation, CAS & MWR (Soil and Water Conservation Project) (A315021304) and (2013KTDZ03-03-01). The author would like to thank Mr. Xiu-quan XU, and Mr. Tong ZHANG for their assistance in experiment processing and Ms. Chun-hong ZHAO, Mr. Hong-jie WANG, Mr. Yuan-xing ZHANG for their advices in writing the paper. At the same time, the authors are very grateful for the editors' and reviewer's hard work in reviewing the paper.

References

Assouline, S., Mualem, Y., 1997. Modeling the dynamics of seal formation and its effect on infiltration as related to soil and rainfall characteristics. Water Resour. Res. 33, 1527–1536.

Athavale, R.N., Chand, R., Rangarajan, R., 1983. Groundwater recharge estimates for two basins in the Deccan Trap basalt formation/Estimation de la recharge des eaux souterraines de deux bassins dans la formation de basalte du Deccan Trap. Hydrol. Sci. J. 28, 525–538.

Athavale, R.N., Rangarajan, R., 1988. Natural recharge measurements in the hard rock regions of semi-arid India using tritium injection—A review. Estimation of Natural Groundwater Recharge. Springer Netherlands. 222, 175–194.

Bowyer-Bower, T.A.S., 1993. Effects of rainfall intensity and antecedent moisture on the steady-state infiltration rate in a semi-arid region. Soil Use Manag. 9, 69–75.

Brandt, C.J., Thornes, J.B., 1987. Erosional energetics. Energetics of Physical Environmentpp. 51–87.

Cerdà, A., Ibáñez, S., Calvo, A., 1997. Design and operation of a small and portable rainfall simulator for rugged terrain. Soil Technol. 11, 163–170.

Cho, J., Barone, V.A., Mostaghimi, S., 2009. Simulation of land use impacts on groundwater levels and streamflow in a Virginia watershed. Agric. Water Manag. 96, 1–11.

Dourte, D., Shukla, S., Singh, P., Haman, D., 2012. Rainfall intensity–duration–frequency relationships for Andhra Pradesh, India: changing rainfall patterns and implications for runoff and groundwater recharge. J. Hydrol. Eng. 18, 324–330.

Dunne, T., Leopold, L.B., 1978. Water in Environmental Planning. WH Freeman.

Eigel, J., Moore, I., 1983a. A simplified technique for measuring raindrop size and distribution. Trans. ASAE 1079–1084.

Eigel, J.D., Moore, I., 1983b. Effect of Rainfall Energy on Infiltration Into a Bare Soil.

Feng, S.Y., Ding, Y.Y., Yao, B., 1998. Study on soil infiltration law with artificial rainfall and numerical simulation. J. Hydraul. Eng. 11, 17–25.

Foley, J.L., Silburn, D.M., 2002. Hydraulic properties of rain impact surface seals on three clay soils—influence of raindrop impact frequency and rainfall intensity during steady state. Soil Res. 40, 1069–1083.

Gädeke, A., Hölzel, H., Koch, H., Pohle, I., Grünewald, U., 2014. Analysis of uncertainties in the hydrological response of a model-based climate change impact assessment in a subcatchment of the Spree River, Germany. Hydrol. Process. 28, 3978–3998.

Gates, J.B., Scanlon, B.R., Mu, X., Zhang, L., 2011. Impacts of soil conservation on groundwater recharge in the semi-arid Loess Plateau. China. Hydrogeol. J. 19, 865–875.

Goel, P.S., Datta, P.S., Rama, S., Prakash Bahadur, S., 1975. Tritium tracer studies on groundwater recharge in the alluvial deposits of Indo-Gangetic Plains of Western UP. Punjab and Haryana, Approaches and Methodologies for Development of Groundwater Resources: Indo-German Workshop, Hyderabad, India, Proceedings, National Geophysical Research Institute. 309–322.

Hawke, R.M., Price, A.G., Bryan, R.B., 2006. The effect of initial soil water content and rainfall intensity on near-surface soil hydrologic conductivity: a laboratory investigation. Catena 65, 237–246.

Hoogmoed, W.B., Stroosnijder, L., 1984. Crust formation on sandy soils in the Sahel I. Rainfall and infiltration. Soil Tillage Res. 4, 5–23.

Horton, R.E., 1919. Rainfall interception. Mon. Weather Rev. 47, 603–623.

Huang, T.M., Pang, Z.H., 2011. Estimating groundwater recharge following land-use change using chloride mass balance of soil profiles: a case study at Guyuan and Xifeng in the Loess Plateau of China. Hydrogeol. J. 19, 177–186.

Huang, J., Wu, P.T., Zhao, X.N., 2012. Effects of rainfall intensity, underlying surface and slope gradient on soil infiltration under simulated rainfall experiments. Catena 104, 93–102.

Hydrogeologic, W., 2005. Visual MODFLOW v. 4.1 User's Manual Waterloo Hydrogeologic Inc. A. Schlumberger Company, Ontario, Canada.

Joel, A., Messing, I., 2001. Infiltration rate and hydraulic conductivity measured with rain simulator and disc permeameter on sloping arid land. Arid Land Res. Manag. 15, 371–384.

Jungerius, P., Ten Harkel, M., 1994. The effect of rainfall intensity on surface runoff and sediment yield in the grey dunes along the Dutch coast under conditions of limited rainfall acceptance. Catena 23, 269–279.

Jyrkama, M.I., Sykes, J.F., Normani, S.D., 2002. Recharge estimation for transient ground water modeling. Groundwater 40, 638–648.

Kim, N.W., Chung, I.M., Won, Y.S., Arnold, J.G., 2008. Development and application of the integrated SWAT–MODFLOW model. J. Hydrol. 356, 1–16.

Kinnell, P., 1981. Rainfall intensity–kinetic energy relationships for soil loss prediction. Soil Sci. Soc. Am. J. 45, 153–155.

LI, G., Huang, G.B., 2009. Effects of rainfall intensity and land use on rainfall and storage in Loess hilly region. Chin. J. Ecol. 28, 2014–2019.

LI, Y.Y., Shao, M.A., 2004. Experimental study on characteristics of water transformation on slope land. J. Hydraul. Eng. 4, 48–53.

Li, F., Zhang, G., Xu, Y.J., 2014. Spatiotemporal variability of climate and streamflow in the Songhua River Basin, northeast China. J. Hydrol. 514, 53–64.

Lin, Q.C., Li, H.E., 2010. Influence and guarantee on ecological basic flow of Weihe River from Baojixia water diversion. J. Arid Land Res. Environ. 24, 114–119.

Lin, R., Wei, K., 2006. Tritium profiles of pore water in the Chinese loess unsaturated zone: implications for estimation of groundwater recharge. J. Hydrol. 328, 192–199.

Liu, C., Chen, L., 2000. Analys is on Runoff Series with Special Reference to Drying up Courses of Lower Huanghe River. Acta Geograph. Sin. 55, 257–265.

Liu, Y., Hu, A.Y., 2006. Changes of precipitation characters along Weihe Basin in 50 years and its influence on water resources. J. Arid Land Res. Environ. 1, 85–87.

Liu, H., et al., 2011. Effects of rainfall intensity and antecedent soil water content on soil infiltrability under rainfall conditions using the run off–on–out method. J. Hydrol. 396, 24–32.

McIntyre, D.S., 1958. Permeability measurements of soil crusts formed by raindrop impact. Soil Sci. 85, 185–189.

Merz, B., Bárdossy, A., Schiffler, G.R., 2002. Different methods for modelling the areal infiltration of a grass field under heavy precipitation. Hydrol. Process. 16, 1383–1402.

Moreno, M.A., Vieux, B.E., 2011. Estimation of Spatio-Temporally Variable Groundwater Recharge Using a Rainfall-Runoff Model. J. Hydrol. Eng. 18, 237–249.

Morin, J., Benyamini, Y., 1977. Rainfall infiltration into bare soils. Water Resour. Res. 13, 813–817.

Owor, M., Taylor, R.G., Tindimugaya, C., Mwesigwa, D., 2009. Rainfall intensity and groundwater recharge: empirical evidence from the Upper Nile Basin. Environ. Res. Lett. 4, 035009.

Rangarajan, R., Deshmukh, S.D., Muralidharan, D., Gangadhara Rao, T., 1989. Recharge estimation in Neyveli ground water basin by Tritium Tagging Method, Technical Report NGRI-89-ENVIRON-65, National Geophysical Research Inst (NGRI), Technical Report NGRI-89-ENVIRON-65.

Ren, L.L., Wang, M.R., Li, C.H., Zhang, W., 2002. Impacts of human activity on river runoff in the northern area of China. J. Hydrol. 261, 204–217.

Richter, B., Baumgartner, J., Wigington, R., Braun, D., 1997. How much water does a river need? Freshw. Biol. 37, 231–249.

Romkens, M.J.M., et al., 1986. Rain-induced surface seals: their effect on ponding and infiltration, Annales Geophysicae. Series B. Terr. Planet. Phys. 4, 417–424.

Salles, C., Poesen, J., Sempere-Torres, D., 2002. Kinetic energy of rain and its functional relationship with intensity. J. Hydrol. 257, 256–270.

Sanford, W., 2002. Recharge and groundwater models: an overview. Hydrogeol. J. 10, 110–120.

Schindewolf, M., Schmidt, J., 2012. Parameterization of the EROSION 2D/3D soil erosion model using a small-scale rainfall simulator and upstream runoff simulation. Catena 91, 47–55.

Schmidt, J., 2010. Effects of soil slaking and sealing on infiltration—experiments and model approach. Proceedings of the 19th World Congress of Soil Science: Soil Solutions for a Changing World, Brisbane, Australia, pp. 29–32.

Scibek, J., Allen, D.M., 2006. Modeled impacts of predicted climate change on recharge and groundwater levels. Water Resour. Res. 42, w11405.

Sharma, P., Gupta, S.K., 1985. Soil water movement in semi-arid climate an isotopic investigation. Stable and Radioactive Isotopes in the Study of the Unsaturated Soil Zone. 60, 55–71.

Shigaki, F., Sharpley, A., Prochnow, L.I., 2007. Rainfall intensity and phosphorus source effects on phosphorus transport in surface runoff from soil trays. Sci. Total Environ. 373, 334–343.

Shu, B.J., Gao, J.E., Wu, P.T., Tian, D., 2006. Test method of raindrop spectrum using plotting software of computer. Sci. Soil Water Conserv. 4, 65–69.

Sophocleous, M., 1993. Comparative review and synthesis of ground water recharge estimates for the Great Bend Prairie aquifer of Kansas. Kansas Geol. Surv. Bull. 235, 41–54.

Sparks, R.E., 1992. Risks of altering the hydrologic regime of large rivers. Predicting Ecosyst. Risk 20, 168–182.

Stone, J.J., Paige, G.B., Hawkins, R.H., 2008. Rainfall intensity-dependent infiltration rates on rangeland rainfall simulator plots. Trans. ASAE 51, 45–53.

Stroosnijder, L., Hoogmoed, W.B., 1984. Crust formation on sandy soils in the Sahel II. Tillage and its effect on the water balance. Soil Tillage Res. 4, 321–337.

Sukhija, B.S., Rama, 1973. Evaluation of groundwater recharge in semi-arid region of India using environmental tritium. Proceedings of the Indian Academy of Sciences A 77, 279–292.

Sukhija, B.S., Shah, C.R., 1976. Conformity of groundwater recharge rate by tritium method and mathematical modelling. J. Hydrol. 30, 167–178.

Sukhija, B.S., et al., 1996. Environmental and injected tracers methodology to estimate direct precipitation recharge to a confined aquifer. J. Hydrol. 177, 77–97.

Tan, X.C., Yang, J.Z., Song, X.H., Zha, Y.Y., 2013. Estimation of groundwater recharge in North China Plain. Adv. Water Sci. 24, 73–81.

Taylor, R.G., Howard, K.W., 1996. Groundwater recharge in the Victoria Nile basin of East Africa: support for the soil moisture balance approach using stable isotope tracers and flow modelling. J. Hydrol. 180, 31–53.

Taylor, R.G., et al., 2013a. Evidence of the dependence of groundwater resources on extreme rainfall in east Africa. Nat. Clim. Chang. 3, 374–378.

Taylor, R.G., et al., 2013b. Ground water and climate change. Nat. Clim. Chang. 3, 322–329.

Van Dijk, A., Bruijnzeel, L., Rosewell, C., 2002. Rainfall intensity–kinetic energy relationships: a critical literature appraisal. J. Hydrol. 261, 1–23.

Wang, H.J., Yang, Z.S., Saito, Y., Liu, J.P., Sun, X.X., 2006. Interannual and seasonal variation of the Huanghe (Yellow River) water discharge over the past 50 years: connections to impacts from ENSO events and dams. Glob. Planet. Chang. 50, 212–225.

Wang, B.G., Jin, M.G., Nimmo, J.R., Yang, L., Wang, W.F., 2008. Estimating groundwater recharge in Hebei Plain, China under varying land use practices using tritium and bromide tracers. J. Hydrol. 356, 209–222.

Wang, H., Gao, J.E., Zhang, S.L., Zhang, M.J., Li, X.H., 2013. Modeling the impact of soil and water conservation on surface and ground water based on the SCS and Visual Modflow. Plos One 8, e79103.

Wang, H., Gao, J.E., Li, X.H., Wang, H.J., Zhang, Y.X., 2014. Effects of Soil and Water Conservation Measures on Groundwater Levels and Recharge. J. Water 6, 3783–3806.

Winder, P., Paulson, K.S., 2012. The measurement of rain kinetic energy and rain intensity using an acoustic disdrometer. Meas. Sci. Technol. 23, 015801.

Wischmeier, W.H., Smith, D.D., 1958. Rainfall energy and its relationship to soil loss. Trans. Am. Geophys. Union 39, 285–291.

Wischmerie, W.H., Smith, D.D., 1979. Predicting rainfall-erosion losses from cropland east of the Rocky Mountains: a guide to conservation planning. Agric. Hardbook. 282, 1–17.

Xu, J., Chen, Y., Li, Q., Nie, Q., Song, C., Wei, C., 2014. Integrating wavelet analysis and BPANN to simulate the annual runoff with regional climate change: a case study of Yarkand River, northwest China. Water Resour. Manag. 9, 2523–2537.

Zhang, H., Hiscock, K.M., 2010. Modelling the impact of forest cover on groundwater resources: a case study of the Sherwood Sandstone aquifer in the East Midlands, UK. J. Hydrol. 392, 136–149.

Zhu, G.F., Li, Z.Z., Su, Y., Ma, J.Z., Zhang, Y.Y., 2007. Hydrogeochemical and isotope evidence of groundwater evolution and recharge in Minqin Basin, Northwest China. J. Hydrol. 333, 239–251.